

# Semiclassical Inequivalence of Polygonalized Billiards

Debabrata Biswas

Theoretical Physics Division, Bhabha Atomic Research Centre, Trombay, Mumbai 400 085, India

Polygonalization of any smooth billiard boundary can be carried out in several ways. We show here that the semiclassical description depends on the polygonalization process and the results can be inequivalent. We also establish that generalized tangent-polygons are closest to the corresponding smooth billiard and for de Broglie wavelengths larger than the average length of the edges, the two are semiclassically equivalent.

Published in Phys. Rev. E 61, 5073 (2000), ©The American Physical Society

## I. INTRODUCTION

Classical billiards are enclosures within which a particle moves freely, and, on collision, reflects specularly from the boundary. The nature of the dynamics thus depends solely on the shape of the enclosure and can vary from integrable motion in case of the circle billiard to hard chaos for the over-lapping 3-disk enclosure. In both these examples, the boundary consists of smooth curves and while these are limiting cases, generic smooth enclosures give rise to intermittent motion. As opposed to such billiards, there exists the category of polygonal billiards where the boundary consists of straight edges alone. These are non-chaotic and generically non-integrable [1,2]. However, any smooth billiard can be *polygonalized* and in more

ways than one. Indeed, such an argument lies at the heart of the discussions in the work of Cheon and Cohen [4] where they consider a polygonal version [5] of the Sinai billiard and observe GOE (Gaussian Orthogonal Ensemble of random matrices) statistics in the level fluctuations [6]. However, there are various other instances of polygonal billiards [8] which exhibit GOE-like fluctuations in a given energy range but do not resemble any chaotic enclosure. Thus, the question of semiclassical equivalence cannot be inferred from such evidence. The work of Tomiya and Yoshinaga [9] is however of greater significance here. They consider polygonalization of the Bunimovich stadium by a generalized tangent construction [10] and observe that apart from statistical measures, several finer features of the stadium are carried over to the tangent polygon. For instance, a Fourier transform of the spectral density reveals a correspondence between the length spectrum of the stadium and the polygon. Besides, individual eigenfunctions in the polygon exhibit scarring, a phenomenon first observed in the stadium billiard [11]. The arguments of Tomiya and Yoshinaga however seem to suggest that the only quantities relevant are  $\lambda$  and  $\Delta l_{max}$  so that there might be little to distinguish between appropriately chosen tangent and step polygons for  $\lambda > \Delta l_{max}$ . In what follows, we shall explore this question in greater detail and attempt to provide an answer.

The paper is organized along the following lines. In section II, we shall deal with the classical aspects of polygonal billiards in general and examine the special features of tangent polygons. In section III, we shall first carry out a semiclassical analysis for generic polygons and then deal with polygonalized billiards. We shall show that generalized tangent-polygons are semiclassically equivalent to smooth polygons while step-polygons are not. A summary of our results and conclusions can be found in section IV.

## II. CLASSICAL DYNAMICS

### A. Polygonal Billiards

A notable aspect of generic polygons is the presence of vertices with internal angles  $\{\pi m_i/n_i\}$ ,  $m_i > 1$ . When,  $m_i = 1$ , the wedge is *integrable* and a parallel band of trajectories continues to remain parallel after an encounter with the wedge. When  $m_i > 1$ , the band splits up and

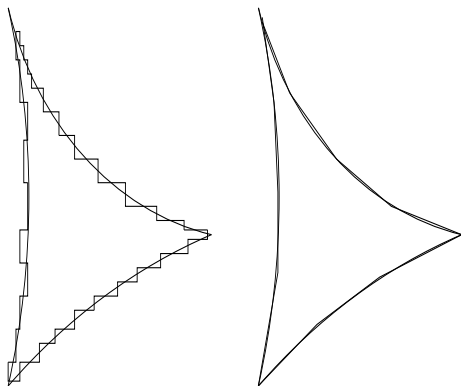


FIG. 1. Two polygonalizations of the 3-disk billiard. We shall refer to the one on the left as the *step-polygon* and the one on the right as the *generalized tangent-polygon* since the edges approximate the local tangents. In case the polygon is formed from the intersection of local tangents, we shall refer to it as a *tangent polygon* (see fig. 4)

Figure 1 shows two ways of approximating a 3-disk enclosure by polygons, and, at the classical level, they are both inequivalent since their invariant surfaces have different topologies (see section II). Let  $\Delta l_{max}$  denote the largest deviation of the step/tangent-polygon from the smooth billiard along the boundary. The question that we shall address here is : *for de Broglie wavelengths,  $\lambda > \Delta l_{max}$ , are these polygons semiclassically equivalent [3] to the smooth billiard ?* Naively, one might expect that they are, since for  $\lambda > \Delta l_{max}$ , the system should be unable to distinguish between the various polygonal-

traverses different paths (see fig. 2). The presence of many such vertices leads to multiple splits in the band as it evolves in time. Interestingly, positive “effective” Lyapunov exponents have been observed in polygonalized billiards [12].

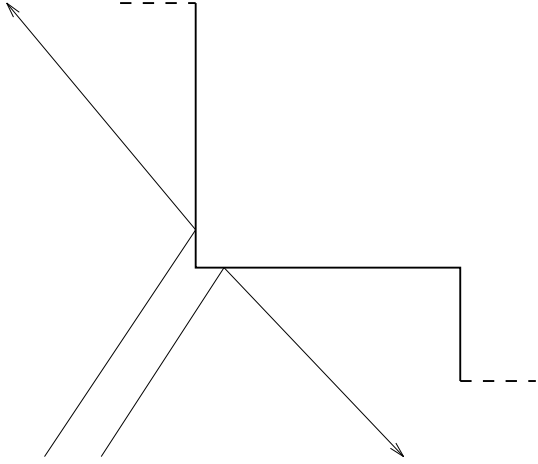


FIG. 2. Parallel rays move away after an encounter with the non-integrable  $(3\pi/2)$  vertex.

The topology of the invariant surface of any polygonal billiard can be determined from its genus,

$$g = 1 + \frac{\mathcal{N}}{2} \sum_i \frac{m_i - 1}{n_i} \quad (1)$$

where  $\mathcal{N}$  is the least common multiple of  $\{n_i\}$  [13]. Thus, for an integrable billiard,  $g = 1$  so that its invariant surface is topologically equivalent to a torus. In the context of polygonalized billiards, it is interesting to note that while for a circle,  $g = 1$ , a polygonalized circle has a very high genus [14]. Also, the step and tangent-polygons of fig. 1 have different genus while the invariant surface of the smooth chaotic billiard is the 3-dimensional constant energy surface.

In any dynamical system, an important set of trajectories are the periodic orbits which live for all times and close in both position and momentum. In case of a billiard, the initial and final velocities are related by a product of reflection matrices, and, for a polygon where the total number of distinct matrices is finite, it is possible to obtain conditions for periodicity in momentum [15]. We shall use the symbols  $\{1, 2, \dots, N\}$  to denote the  $N$  sides of the polygon and label trajectories by a string of symbols  $s_1 s_2 \dots s_n$  where  $s_i \in \{1, 2, \dots, N\}$ . Thus a sequence 1323 denotes a trajectory that reflects off sides 1, 3, 2 and 3 respectively. Let us denote by  $R_i, i = 1, N$  the  $2 \times 2$  reflection matrices of the  $N$  sides. These can be expressed in terms of the angle  $\theta_i$  between the outward normal to a side and the positive  $X$ -axis :

$$R_i = \begin{pmatrix} -\cos(2\theta_i) & -\sin(2\theta_i) \\ -\sin(2\theta_i) & \cos(2\theta_i) \end{pmatrix}. \quad (2)$$

Thus, for the sequence 1323, the initial and final velocities are related by

$$\begin{pmatrix} v_x^f \\ v_y^f \end{pmatrix} = R_3 \circ R_2 \circ R_3 \circ R_1 \begin{pmatrix} v_x^i \\ v_y^i \end{pmatrix} = R_{1323} \begin{pmatrix} v_x^i \\ v_y^i \end{pmatrix} \quad (3)$$

where the superscripts  $f$  and  $i$  refer respectively to the final and initial velocity whose components are  $v_x$  and  $v_y$ . It is easy to verify that when the number of reflections is odd

$$R_{s_1 s_2 \dots s_n}^{(odd)} = \begin{pmatrix} -\cos(\varphi_o) & -\sin(\varphi_o) \\ -\sin(\varphi_o) & \cos(\varphi_o) \end{pmatrix} \quad (4)$$

where  $\varphi_o = 2(\theta_1 + \theta_3 + \dots + \theta_n) - 2(\theta_2 + \theta_4 + \dots + \theta_{n-1})$  while for even number of reflections ( $n$  even)

$$R_{s_1 s_2 \dots s_n}^{(even)} = \begin{pmatrix} \cos(\varphi_e) & \sin(\varphi_e) \\ -\sin(\varphi_e) & \cos(\varphi_e) \end{pmatrix} \quad (5)$$

where  $\varphi_e = 2(\theta_1 + \theta_3 + \dots + \theta_{n-1}) - 2(\theta_2 + \theta_4 + \dots + \theta_n)$ .

Obviously, the initial and final velocities can be equal if the resultant reflection matrix  $R_{s_1 s_2 \dots s_n}$  has a unit eigenvalue. For even  $n$  (the case of bands or families), the eigenvalues are  $e^{\pm i\varphi_e}$  so that the condition for the existence of a unit eigenvalue is

$$\varphi_e = 0 \pmod{2\pi}. \quad (6)$$

For odd  $n$  on the other hand, the product of the eigenvalues  $\lambda_1 \lambda_2 = 1$ . The eigenvector corresponding to a unit eigenvalue is  $(\sin(\varphi_o/2), -\cos(\varphi_o/2))$  so that if a real orbit exists with the sequence  $s_1 s_2 \dots s_n$ , its initial and final velocities are equal.

In the event that a sequence repeats itself (denoted by  $\overline{s_1 s_2 \dots s_n}$ ) and there exists a unit eigenvalue of the resultant matrix  $R_{s_1 s_2 \dots s_n}$ , stability considerations guarantee that a periodic orbit exists. To see this, consider first an odd bounce orbit ( $n$  odd) for which  $s_{n+1} = s_1$  and the initial and final velocities are equal. Assume further that the initial and final segments of the trajectory are separated by a distance  $d$  along the edge,  $s_1$ . It is then easy to verify that an isolated periodic orbit exists exactly in between the two segments (i.e. at a distance  $d/2$  from either segment) with the same velocity. For the even  $n$  case, note first that eq. (6) does not select a particular eigenvelocity. In other words, there is a range of initial velocities for which (i)  $s_1 = s_{n+1}$ , (ii) the trajectory follows the same sequence  $s_1 s_2 \dots s_n$  and (iii) the initial and final velocities are equal. For convenience, assume as before that the trajectory starts from edge  $s_1$ , encounters  $n$  bounces and reflects off the same edge after traversing a length,  $l$ , to become parallel to the initial segment. Further, assume that the two parallel segments are separated by a distance  $d$ . It then follows that a periodic family exists with a velocity correction,  $\Delta\phi \simeq d/l$ . In practice, one can rapidly converge to the correct angle after a few corrections [16,17].

We have thus obtained conditions for the existence of periodic orbits in polygonal enclosures. Note that in the neighbourhood of every polygon,  $P^i$ , for which a sequence  $s_1 s_2 \dots s_n$  yields a periodic family, there exists an infinity of polygons for which this sequence results in a closed almost-periodic (CAP) family of orbits [15]. These orbits

close in position but the angle,  $\varphi_e$ , between the initial and final momentum (at the point where the orbit closes) is non-zero but small. In contrast,  $\varphi_e = 0$  for periodic families. CAP orbit families play a special role in the classical dynamics of tangent-polygons as we shall now show.

### B. Tangent Polygons

We shall deal with a (generalized) tangent-polygon consisting of  $N$  edges which approximates a chaotic 3-disk billiard as shown in fig. 1. Individual edges thus have an average length  $l_{av} = \mathcal{L}/N$  where  $\mathcal{L}$  is the perimeter of the smooth billiard. We shall show here that for  $N$  sufficiently large, the neighbourhood of isolated periodic orbits in the smooth billiard is well approximated by (i) closed almost-periodic families of the tangent-polygon for even  $n$  and (ii) isolated marginally stable periodic orbits together with the closed orbits in their neighbourhood for odd  $n$ .

Consider thus an unstable isolated periodic orbit in the smooth 3-disk billiard with symbol sequence  $\overline{s_1 s_2 \dots s_n}$  where  $s_j \in \{1, 2, 3\}$  corresponding to the 3 sides and  $n$  is the number of bounces or the topological length of the trajectory. Associated with this periodic orbit is a cylinder of extent  $J_i^{(n)}$  within which all orbits follow the same symbol sequence [18,19]. Obviously,  $J_i^{(n)}$  depends on the stability and the length of the periodic orbit. In the corresponding tangent-polygon, if  $n$  is reasonably small ( $n < n_{max}$ ) and  $N$  large ( $n_{max} = n_{max}(N)$ ), most trajectories in the cylinder survive the sequence in which the polygonalized disks are visited [20]. Note that corresponding to every isolated periodic orbit in the smooth billiard, there exists a set of  $n$  tangents (at the points of impact) off which the orbit reflects. In the unlikely event that the tangent polygon has exactly this set as its edges, a periodic orbit trivially exists in the polygonalized billiard as well. In general however, the set of tangents can only be *approximated* by one or more sets of edges in the polygon.

Consider, first the case when  $n$  is even. Clearly, for any [21] set of edges that preserves the sequence in which the polygonalized disks are visited,  $\varphi_e \neq 0$  and hence a periodic orbit family does not exist. However, if the approximation is good,  $\varphi_e$  will be small so that a closed almost-periodic family exists where the angle between the initial and final momentum is  $\varphi_e$ . Within this family, the difference in length of two orbits is  $\varphi_e q_\perp$  where  $q_\perp$  is the transverse separation between the two [15]. Thus, if  $\varphi_e$  is small, the variation in length within the family is slow. In general, there can be more than a single set of such closed almost-periodic family depending on  $N$  and the stability of the isolated periodic orbit and for one of these, the average length will be close to that of the isolated periodic orbit. The variation in length of closed almost-periodic orbits is schematically shown in fig. 3 (case a) where the dashed curve describes the neighbourhood of the isolated periodic orbit. Clearly, with an increase in

$N$ , the number of families increase, their widths decrease and the approximation of the neighbourhood by closed almost-periodic families gets better.

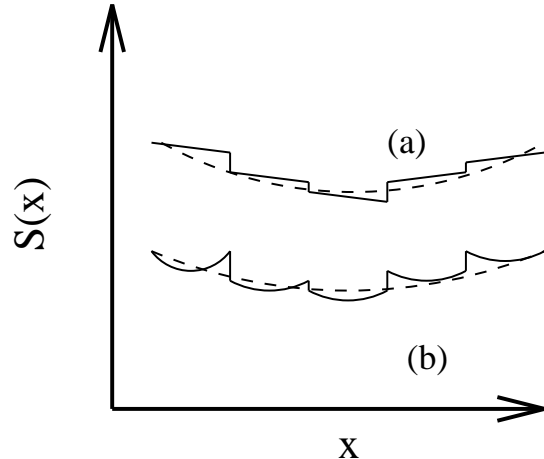


FIG. 3. Schematic variation of the action,  $S(x)$ , in the transverse direction,  $x = q_\perp$  for (a) even  $n$  closed almost-periodic families and (b) odd  $n$  closed orbits in the tangent polygon.

For the case of odd  $n$ , assume that an isolated unstable periodic orbit exists for the sequence  $s_1 s_2 \dots s_n$  in the smooth billiard with an initial velocity that can be calculated from the set of tangents to the boundary at the points of impact. For every set (of edges) that approximates these tangents, there exists in the polygon an isolated marginally stable periodic orbit with a slightly different initial velocity owing to the difference in  $\varphi_e$ . On either side however, there exist closed orbits that follow the same sequence and whose length increases as  $l(q_\perp) = l(0) [1 + (2q_\perp/l(0))^2]^{1/2}$  where  $l(0)$  is the length of the periodic orbit and  $q_\perp$  measures the transverse distance from it. As before, for every set of edges that approximates the tangents, one can observe this behaviour so that the variation in length in the neighbourhood of the unstable isolated periodic orbit is schematically as shown in fig. 3 (case (b)).

Apart from the closed almost-periodic orbits, there exist an infinite number of exact periodic orbit families in every polygonalized billiard. The extent of these families is limited by the length of the smallest edge and within each such family, periodic orbits have identical length. For  $N$  sufficiently large however, along with every set of edges that gives rise to an exact periodic family, there exist other sets of edges for which orbits follow the same sequence but are almost-periodic. The variation in length is thus only marginally different from that shown schematically in fig. 3 (case a) with one band having constant length while in the others, the length changes linearly within the band.

### C. Step Polygons etc.

We now turn our attention to the step polygon of fig. 1. Obviously, the edges do not locally approximate the tangent at any point of the smooth billiard so that the cylinder  $J_i^{(n)}$  does not survive even for small  $n$ . In fact, there exist several families of bouncing ball orbits in the step polygon of fig. 1 which have no correspondence in the smooth billiard. Besides, all periodic orbits have even  $n$  and closed almost-periodic families do not exist in this case. Thus the classical dynamics in the neighbourhood of isolated unstable periodic orbits is not approximated by closed orbits in the step polygon.

There are several other methods of polygonalizing smooth billiards and in each of these, the symbolic dynamics of the smooth billiard cannot survive unless the edges locally approximate the tangents. In summary then, generalized tangent polygons are the only systems in which the classical dynamics of smooth billiards is locally preserved for  $n < n_{max}$ .

## III. SEMICLASSICS

### A. Generic Polygons

Having established a correspondence between the classical dynamics of the smooth billiard and the tangent polygon, we shall now consider the quantum problem and derive a semiclassical expression for its density of states. The starting point in such an analysis is the relation [22]

$$\sum_n \frac{1}{E - E_n} = \int dq G(q, q; E) \quad (7)$$

$$\simeq \int dq G_{s.c.}(q, q; E) \quad (8)$$

where  $\{E_n\}$  are the energy eigenvalues and  $G_{s.c.}$  refers to the semiclassical energy dependent propagator (Green's function). For a polygonal billiard,

$$G_{s.c.}(q, q'; E) = -i \sum \frac{1}{\sqrt{8\pi i k l(q, q')}} e^{ikl(q, q') - i\mu\pi/2} \quad (9)$$

where the sum runs over all orbits at energy  $E = k^2$  between  $q$  and  $q'$  having length  $l(q, q')$  and  $\mu$  is twice the number ( $n$ ) of reflections at the boundary. For convenience, we have chosen the mass  $m = 1/2$  and  $\hbar = 1$

In the limit  $k \rightarrow \infty$ , the only trajectories that survive the trace operation are the periodic orbits [22]. As mentioned earlier, even bounce periodic orbits occur in families over which the length of the orbit does not vary and for these  $\int dq = a_p$  where  $a_p$  refers to the area occupied by a primitive periodic orbit [23]. For the odd-bounce case, a local co-ordinate system  $(q_{\parallel}, q_{\perp})$  needs to be introduced where  $q_{\parallel}$  is the position along the isolated periodic orbit and  $q_{\perp}$  measures the transverse distance from the periodic orbit. Since the length does not vary along the orbit,  $\oint q_{\parallel} = l_{p'}$  where  $l_{p'}$  is the length of the

primitive periodic orbit. The  $q_{\perp}$  integration can be performed by the stationary phase approximation using the expression for  $l(q_{\perp})$  given earlier. Thus,

$$\begin{aligned} \rho(E) &= \sum_n \delta(E - E_n) = -\frac{1}{\pi} \lim_{\epsilon \rightarrow 0} \Im \frac{1}{E + i\epsilon - E_n} \\ &\simeq \rho_{av}(E) + \sum_p \sum_{r=1}^{\infty} \frac{a_p}{\sqrt{8\pi^3 k r l_p}} \\ &\quad \times \cos(kr l_p - \pi/4) - \sum_{p'} \sum_{r'=1}^{\infty} \frac{l_{p'}}{4\pi k} \cos(kr' l_{p'}). \quad (10) \end{aligned}$$

where  $\rho_{av}$  is the average density of states and the sums over  $p$  and  $p'$  run over (primitive) *families* and isolated orbits respectively having length  $l_p$  and  $l_{p'}$ .

For finite  $k$  however, eq. (10) is inadequate for generic polygons and the most prominent correction that has so far been taken into account arises from diffraction [24–26]. It has recently been shown [15] that closed almost-periodic orbit families contribute as well and with weights comparable to those of periodic orbit families when  $\varphi_e$  is small. The correct trace formula can be derived by noting that for a closed almost-periodic family,  $l(q_{\perp}) = l(0) + q_{\perp} \varphi_e$  where  $l(0) = l_i$  is the length of the orbit in the centre of the band and  $q_{\perp}$  varies from  $-w_p/2$  to  $w_p/2$ . Assuming that  $k$  is sufficiently large, the amplitude ( $1/l(q_{\perp})$ ) can be treated as a constant ( $1/l_i$ ) and the trace formula for finite  $k$  is then

$$\begin{aligned} \rho(E) &\simeq \rho_{av}(E) + \sum_i \frac{a_i}{\sqrt{8\pi^3 k l_i}} \\ &\quad \times \cos(k l_i - \pi/4) \frac{\sin(k \varphi_e^{(i)} w_i/2)}{k \varphi_e^{(i)} w_i/2} \\ &\quad - \sum_{p'} \sum_{r'=1}^{\infty} \frac{l_{p'}}{4\pi k} \cos(kr' l_{p'}). \quad (11) \end{aligned}$$

In eq. (11), the sum over  $i$  runs over closed almost-periodic and periodic orbit families and  $l_i$  is the (average) length of such a family. Note that as  $k \rightarrow \infty$ , the contribution of CAP families ( $\varphi_e^{(i)} \neq 0$ ) vanishes and eq. (11) reduces to eq. (10). For de Broglie wavelength,  $\lambda \gg \pi(w_p \varphi_e^{(i)})$ , however, the ( $i$ th) closed almost-periodic orbit family contributes with a weight comparable to that of periodic families ( $\mathcal{O}(1/k^{1/2})$ ) and hence assumes greater significance than diffraction. Interestingly, such orbits clearly show up in eigenfunctions [27] and the phenomenon has been referred to as “scarring by ghosts of periodic orbits” since such a periodic orbit exists only in a neighbouring polygon.

Note that almost-periodic closed orbit families do not generally occur in systems where the number of directions accessible to a trajectory is small since the (average) angle of intersection is large. Thus in step billiards or in systems with very low genus, almost-periodic families do not contribute significantly. In generic polygons however, these orbits are the key to semiclassical quantization.

## B. Tangent Polygons

Though eq. (11) holds for generic polygons, we shall use a somewhat different approach for the tangent-polygons where several families of closed almost-periodic families exist together with a gradual change in length. This variation can be approximated by a smooth curve as depicted schematically in fig. 3. For  $N$  sufficiently large, it is reasonable to choose the smooth curve as the one which describes the (linearized) neighbourhood of the isolated unstable periodic orbit in the chaotic billiard and the error so introduced can be evaluated. Thus instead of summing over nearby bands we shall carry out a single integration for every periodic sequence. The trace operation then leads to the truncated Gutzwiller trace formula

$$\rho(E) \simeq \rho_{av}(E) + \frac{1}{k} \left[ \sum_{T_p < T^*} \sum_{r=1}^{\infty} \frac{l_p}{2\pi \sqrt{|\det(J_p^r - I)|}} \times \cos(krl_p - r\mu_p\pi/2) + \Delta\rho_1 + \Delta\rho_2 \right] \quad (12)$$

with errors  $\Delta\rho_1$  and  $\Delta\rho_2$ . In eq. (12),  $T_p = l_p/2k$  is the time period of a primitive periodic orbit,  $J_p$  is the Jacobian matrix arising from a linearization of the flow in the neighbourhood of a periodic orbit and  $\mu_p$  is the Maslov index associated with the primitive orbit.

Of the errors, the first,  $\Delta\rho_1$ , arises due to the restriction of the periodic orbit sum to orbits of length  $T_p < T^*$  since the correspondence between the smooth billiard and the tangent polygon exists only for  $n < n_{max}$ . Obviously,  $\lim_{N \rightarrow \infty} \Delta\rho_1 = 0$ . We shall however consider tangent polygons for which  $T^* > T_H$  ( $T_H$  is the Heisenberg time) such that the energy eigenvalues evaluated using the truncated periodic orbit sum gives a faithful approximation to the true eigenvalues  $\{E_n\}$ . Thus, we shall neglect  $\Delta\rho_1$  henceforth.

The error  $\Delta\rho_2$  arises due to the approximation shown in fig. 3 and a crude estimate of this can be obtained by assuming that the length is constant within a band. The error is then

$$\Delta\rho_2 \simeq \sum_i \frac{w_i^2}{2} f'(x_i) \quad (13)$$

where  $w_i$  is the width of the  $i$ th band,  $x_i$  is the value of  $q_{\perp}$  within the  $i$ th band for which  $l(q_{\perp})$  equals the value of the smooth curve and

$$f(q_{\perp}) \sim k^{1/2} e^{ikl(q_{\perp})} \quad (14)$$

Thus,

$$\Delta\rho_2 \sim \sum_i w_i^2 k^{3/2} \sim l_{av}^2 k^{3/2} = \frac{\mathcal{L}^2 k^{3/2}}{N^2} \quad (15)$$

In writing the above we have used the facts that the maximum width,  $w_i$  of a periodic orbit band is limited by the average length,  $l_{av}$  of the edges. We may further assume that the number of families corresponding to a

cylinder  $\bar{J}_i^{(n)}$  is small compared to  $N$  so that  $\Delta\rho_2 \sim k^{3/2}/N^2$ . Thus for  $k \ll \mathcal{C}N^{4/3}$ , the tangent polygon is semiclassically equivalent to the smooth billiard where  $\mathcal{C}$  is a positive constant which depends on the exact form of  $f(x)$ .

It may be noted that a special construction of tangent polygon occurs in the boundary integral method of evaluating quantum eigenvalues. Here, the Schroedinger equation is reduced to an eigenvalue problem for an integral operator  $K$  [28]

$$\psi(s) = \oint ds' \psi(s') K(s, s'; k) \quad (16)$$

$$K(s, s'; k) = -\frac{ik}{2} \cos \theta(s, s') H_1^{(1)}(k|\vec{s} - \vec{s}'|) \quad (17)$$

$$\cos \theta(s, s') = \hat{n}(\vec{s}) \cdot \hat{\rho}(s, s') \quad (18)$$

where  $E = k^2$ ,  $\hat{\rho}(s, s') = (\vec{s} - \vec{s}')/|\vec{s} - \vec{s}'|$  and  $\hat{n}(\vec{s})$  is the outward normal at the point  $\vec{s}$ . The unknown function is now the normal derivative on the boundary

$$\psi(s) = \hat{n}(\vec{s}) \cdot \nabla \Psi(\vec{s}) \quad (19)$$

and the full interior eigenfunction can be recovered through the mapping

$$\Psi(q) = -\frac{i}{4} \oint ds H_0^{(1)}(k|\vec{s} - \vec{s}'|) \psi(s). \quad (20)$$

In practice, the boundary is discretized with the number of points  $N \simeq \mathcal{L}k/\pi$  [29]. Eq. (16) then reduces to a matrix equation leading to the consistency condition

$$\det(I - \Delta l K(k)) = 0 \quad (21)$$

where  $\Delta l$  is the incremental distance along the boundary and  $I$  is the identity matrix. Note that for a straight edge,  $K_{nn} = 0$  while for a curved boundary,  $K_{nn} = \pm 1/(2\pi R_n)$  where  $R_n$  is the local radius of curvature at the boundary point  $s_n$  and the + and - signs are for convex and concave boundaries respectively.

The corresponding tangent polygon may be constructed by the intersection of the tangents at the boundary points  $s_n$  as shown in fig. 4 and this in turn may be solved

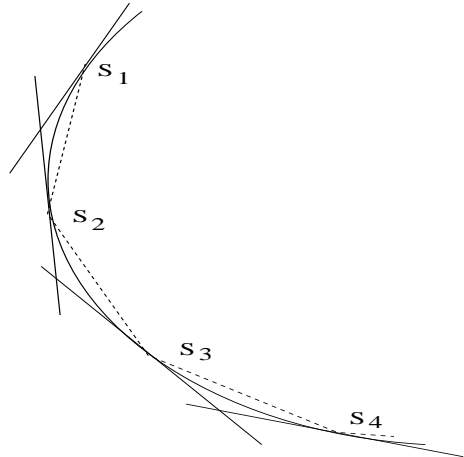


FIG. 4. Construction of a polygon using the tangents at the points  $\{s_n\}$ .

using the boundary integration method with the same set of points  $\{s_n\}$ . The only difference then would be the local curvature in the diagonal matrix element, which for any polygon is zero. The error so generated is similar to the approximation of fig. (3) where we replace the steps by a smooth curve which contains information about the local curvatures at the points of impact.

To test this assertion, we have evaluated the eigenvalues using the boundary integral method for an intersecting 3-disk system with (a)  $K_{nn} = 0$  in one case and (b)  $K_{nn} = 1/(2\pi R_n)$  in the other. In both cases,  $N = 2\mathcal{L}k/\pi$  where  $\mathcal{L} = 1$ . Table I lists the four sets of eigenvalues in the range  $1505 < k < 1506$ . The first two are the exact quantum eigenvalues for the 3-disk and the tangent-polygon ( $K_{nn} = 0$ ) while the eigenvalues in the third and fourth columns are determined using the asymptotic form of the Hankel function,  $H_1^{(1)}$  and are referred to as the “semiclassical” eigenvalues [29]. Clearly, the polygonalization error is small compared to the semiclassical error so that the two systems are equivalent.

### C. Circles , Step Polygons etc.

It is easy to see that the analysis carried out so far holds for other smooth billiards which are non-chaotic and where periodic orbits may occur in families. An extreme case is the circle billiard where under similar conditions, a one to one correspondence between its periodic orbits and those of the tangent polygon exists. However, rather than a single family of periodic orbits with a sharply defined action and angular momentum, there exists in the tangent polygon, a number of closed almost-periodic bands (or isolated periodic orbits and the associated closed orbits in its neighbourhood when  $n$  is odd). When the variation in length across these families is small ( $N$  large), it can be replaced by a constant length typical of periodic orbit families and the error so generated can be similarly evaluated.

In case of the step polygon of fig. 1, only the Weyl term in the density of states agrees with that of the 3-disk billiard as the areas can be made identical in an appropriate construction. The contributions from periodic orbits are bound to differ as explained in section II and diffractive corrections are both significant and different from those in the 3-disk. Thus, the two systems are inequivalent.

## IV. CONCLUSIONS

We have addressed the question of semiclassical equivalence of polygonalized billiards in this paper and in the process analyzed the conditions under which orbits are periodic in generic polygons. We have also provided a trace formula for finite energy that includes contributions from closed almost-periodic orbit families. Since their weights can be comparable to those of periodic orbit families, such orbits must be included in any realistic semiclassical calculation.

In summary, polygonalized billiards are *semiclassically* equivalent to smooth billiards in appropriate energy ranges only when the edges locally approximate the tangents to the boundary of the smooth billiard. In other cases such as the step polygon, the classical dynamics has no correspondence with the smooth billiard and the two are not semiclassically equivalent.

The results of this paper can be applied to statistics of quantum energy levels with interesting consequences and we shall briefly discuss these here. It is obvious that given any smooth billiard, there exist tangent polygons whose energy levels faithfully approximate those of the smooth billiard in a range that increases with the number of sides in the polygon. Thus, the level statistics in this range can vary from Poisson to GOE depending on the statistics of the smooth billiard. At finite energies therefore, polygonal billiards do not belong to any universality class. This however does not preclude the existence of universality in a sub-class of polygons such as generic triangular billiards. It also follows that level statistics at finite energies does not depend on the genus within the broad class of polygons.

- 
- [1] A.N. Zemlyakov and A.B. Katok, Math. Notes, **18**, 760 (1976); *ibid* **20**, 1051 (1976).
  - [2] E. Gutkin, J. Stat. Phys. **83** 7 (1996).
  - [3] In this paper, two billiards are said to be semiclassically equivalent if their leading order contributions to the semiclassical trace formula are identical. The semiclassically quantized energy levels are thus identical.
  - [4] T. Cheon and T. D. Cohen, Phys. Rev. Lett. **62**, 2769 (1989).
  - [5] The circle is approximated by steps in this case.
  - [6] The quantum energy eigenvalues are known to obey *GOE* statistics when the corresponding classical system is chaotic [7].
  - [7] O. Bohigas, M.-J. Giannoni and C. Schmit, Phys. Rev. Lett. **52**, 1 (1984).
  - [8] D. Biswas, Phys. Rev. E **57**, R3699 (1998).
  - [9] Tomiya and Yoshinaga J. Stat. Phys. **85**, 215 (1996).
  - [10] In order to preserve area, the edges that replace the semi-circles are not tangents. We shall use the term “generalized tangent-polygon” in all cases where the edges approximate the local tangents to the smooth billiard.
  - [11] E. J. Heller, Phys. Rev. Lett. **53**, 1515 (1984).
  - [12] J. L. Vega, T. Uzer and J. Ford, Phys. Rev. E **48**, 3414 (1993); see also G. Mantica, *Quantum algorithmic integrability: the metaphor of polygonal billiards*, [chaos-dyn/9906018](https://arxiv.org/abs/chaos-dyn/9906018).
  - [13] A surface with genus,  $g$ , is topologically equivalent to a sphere with  $g$  holes.
  - [14] For computational purposes, we shall assume that the internal angles are rational multiples of  $\pi$ . Irrational polygons are ergodic in a measure theoretic sense; see for instance R.Artuso, G.Casati and I.Guarneri, Phys. Rev. E **55** (1997) 6384 and references therein.

- [15] D. Biswas, [chao-dyn/9909010](https://arxiv.org/abs/chao-dyn/9909010).
- [16] D. Biswas, Phys. Rev. E **54**, R1044 (1996).
- [17] D. Biswas, Pramana, J. Phys. **48**, 487 (1997).
- [18] P. Cvitanović, et al., *Classical and Quantum Chaos*, <http://www.nbi.dk/ChaosBook/>, (Niels Bohr Institute, Copenhagen, 1999).
- [19] The subscript  $i$  refers to one of the several distinct periodic sequences having symbol length  $n$ .
- [20] A trajectory cannot successively visit two edges from the same polygonalized disk.
- [21] There can be more than a single set of edges for which the symbol sequence is the same depending on  $N$  and the stability of the periodic orbit in the smooth billiard.
- [22] M. C. Gutzwiller, *Chaos in Classical and Quantum Mechanics* (Springer Verlag, New York, 1990); in *Chaos and Quantum Physics*, Les Houches 1989, eds. M.-J. Giannoni, A. Voros and J. Zinn-Justin, North Holland, 1991.
- [23] P. J. Richens and M. V. Berry Physica D **2**, 495 (1981).
- [24] N. Pavloff and C. Schmit Phys. Rev. Lett. **75**, 61 (1995).
- [25] H. Bruss and N. D. Whelan, Nonlinearity, **9**, 1023 (1996).
- [26] M. Sieber, N. Pavloff and C. Schmit, Phys. Rev. E **55**, 2279 (1997).
- [27] P. Bellomo and T. Uzer, Phys. Rev. E **50**, 1886 (1994).
- [28] P. A. Boasmann, *Ph.D thesis*, unpublished.
- [29] E. B. Bogomolny, Nonlinearity **5**, 805 (1992).

$k_{3disk}^{exact}$	$k_{polygon}^{exact}$	$k_{3disk}^{semi}$	$k_{polygon}^{semi}$
1505.11325	1505.11324	1505.16810	1505.16809
1505.17526	1505.17527	1505.24944	1505.24945
1505.37518	1505.37518	1505.43624	1505.43624
1505.49791	1505.49792	1505.55890	1505.55890
1505.59969	1505.59969	1505.65119	1505.65119
1505.72383	1505.72382	1505.78927	1505.78926
1505.77798	1505.77798	1505.83193	1505.83192
1505.83710	1505.83709	1505.89083	1505.89082

TABLE I. A comparison of the exact and semiclassical eigenvalues of the 3-disk with the exact and semiclassical eigenvalues of the corresponding tangent polygon. Neglect of the curvature term makes little difference compared to the semiclassical approximation.